

Clawpole Transverse Flux Machines with Amorphous Stator Cores

Nicolas Dehlinger, Student Member IEEE, Maxime R. Dubois, Member IEEE.
e-mail: nicolas.dehlinger.1@ulaval.ca

Abstract- The use of an hybrid stator, made of a combination of Fe-Si laminations and Soft Magnetic Materials (SMC), has been recently proposed to reduce the iron losses occurring in a Clawpole Transverse Flux Machine (CTFM). In this paper, we show that a very low-loss magnetic material, the amorphous material, can be easily used as a substitution to the Fe-Si laminations to reduce the losses further. The stator iron losses in a CTFM with amorphous cores are compared to those occurring in a CTFM with Fe-Si cores by experimental tests and finite element simulations. It is found that the use of amorphous cores could increase the machine efficiency and speed range.

I. INTRODUCTION

Transverse flux machines (TFMs) have the potential of higher power and torque densities when compared to conventional DC, synchronous and induction machines [1]. For example, such a machine can achieve power densities that are three times higher than those of an induction machine with similar power rating and efficiency [2]. For this reason, TFMs look very attractive to some low-speed direct-drive applications such as wind turbine generators or traction motors for electric vehicles as stated in [3].

In conventional machines, also referred as longitudinal flux machines, main flux paths lay in planes parallel to the direction of motion. In the case of TFMs, flux lines mainly remain in planes perpendicular to the direction of motion due to a particular magnetic arrangement (Fig 1). As explained by Weh in [1], TFMs unusual magnetic circuit explains the high power and torque capabilities of such machines: this particular arrangement allows increasing their pole number without reducing their magnetomotive force per pole.

Despite their advantages, TFMs also have some serious shortcomings like low power factor, complex construction and high cost [1-5]. Moreover, the TFM shows a dependence of its force density upon its pole pitch and airgap thickness. High torque density is usually obtained with a very short pole pitch (5 – 20 mm), which leads to high electrical frequencies and thus to high core losses [6]. For example, a 30-pole TFM

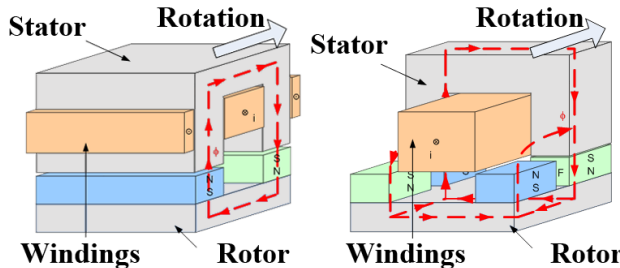


Fig 1: Main flux paths (dashed) in a stator pole pair of a (left) longitudinal and (right) transverse flux machine.

running at 1800 rpm will have an electrical frequency of 450 Hz. As the pole number increases, high iron losses often limit the machine rotational speeds to avoid cooling difficulties or to prevent a decrease of the motor efficiency [5] [6].

Since the introduction of the transverse flux concept by Weh in 1986 [1], multiple geometries have emerged: TFMs with either active or passive rotor, single- or double-sided machines, TFM with surface magnets or with flux-concentration. The aim of this document is not to present the advantages of all existing TFM geometries as it is already well documented in the literature like in [3]. This paper focuses on a particular type of TFM: the Clawpole TFM (CTFM) [4] (Fig 2). Among all existing TFM structures, the CTFM seems to offer the best compromise in terms of torque density and ease of construction and manufacturing [6]. Because of 3D magnetic flux paths and unusual core shapes, it is difficult to build a CTFM using conventional electrical steel laminations. Soft Magnetic Composites (SMC) are usually preferred, offering isotropic magnetic properties and easier manufacturing [4]. Even though SMC have been substantially improved in the last years, their specific iron losses are still higher than those of conventional Fe-Si laminations. Despite its high torque density and manufacturing advantage, CTFMs still suffer from high iron losses that the use of SMC may worsen.

A solution to reduce the iron losses in a CTFM was proposed in [6] by the using a "hybrid stator" made of a combination of Fe-Si laminations and SMC. In this paper, the concept of hybrid stator is further developed by using new magnetic materials with lower specific losses: amorphous magnetic materials. Experimental measurements and finite element simulations were made to quantify the iron loss reduction in a CTFM with amorphous stator cores.

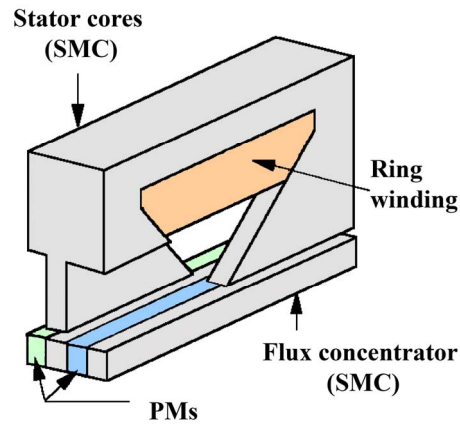


Fig 2: One pole pair of a Clawpole TFM [4].

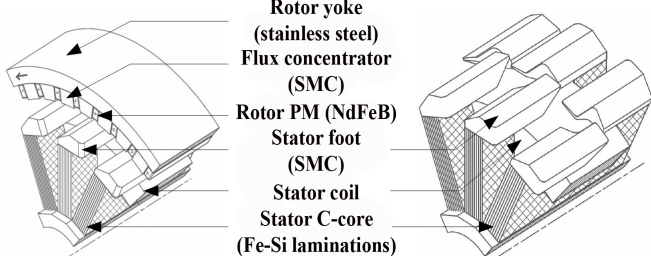


Fig 3: CTFM with hybrid stator (3 pole pairs of 1 phase) [6].

II. CLAWPOLE TFM WITH HYBRID STATOR

In [6], a solution for the reduction of iron losses in the CTFM is proposed: the stator core is split in 2 parts: laminated C-cores and SMC stator feet (Fig 3). The use of an isotropic material like SMC in the stator feet is necessary because of high 3D magnetic flux paths. For the stator C-cores, laminated material can be used, the flux path being mainly 2D. This configuration of TFM is called "CTFM with hybrid stator" referring to the use of 2 different materials for the stator.

With help of 3D Finite Element Analysis (FEA) simulation tools, the iron losses occurring in a 3 phases, 10 kW, 15 pole pairs CTFM with Fe-Si C-cores (hybrid stator) were compared to the losses in a similar CTFM with SMC C-cores: Dubois *et al.* concluded to a 55 % of iron losses reduction in the C-cores of the hybrid stator machine at 900 rpm (225 Hz) [6]. Experimental measurements made on a prototype with Fe-Si cores, with the same dimensions as the one simulated, showed a motor efficiency of 93 % at 240 rpm (60 Hz).

The stator segmentation and the use of SMC in the regions contiguous to the airgap also improves manufacturing by: (1) allowing easier winding of the stator coil, (2) enabling the use of conventional stamping methods for the C-cores laminations, and (3) allowing both rotor and stator machinability leading to very thin airgaps (0.55 mm).

In brief, the concept of hybrid stator presented in [6] enables reducing the CTFM iron losses while also simplifying the machine construction and manufacturing. In the next section, the concept of hybrid stator is further developed by using new magnetic materials with lower specific losses. The substitution of the Fe-Si lamination cores by amorphous ones is presented in the following sections.

III. AMORPHOUS MAGNETIC MATERIALS

Metal alloys, such as Fe-Si alloys, typically have periodically ordered crystalline atomic structures. Amorphous metal alloys, also frequently referred to as metallic glasses, possess particular atomic structures in which the atoms are arranged in near random configurations. According to [8] and [9], amorphous alloy compositions typically contain 75 – 85 % of transition metal elements (Fe, Co, Ni) combined to 15 – 25 % of metalloids (B, C, Si, P). By being quenched from liquid state very rapidly, amorphous alloys avoid the equilibrium crystalline atomic structure retaining the disordered structure of a glass [8]. Thanks to near random atomic arrangements, metallic glasses distinguish from other alloys by excellent

TABLE I
MAGNETIC PROPERTIES OF VARIOUS METGLAS® AMORPHOUS ALLOYS.

Alloy name	Saturation induction [T]	Maximum permeability	Specific iron losses [W/kg]
Fe-rich alloys			
Metglas 2605SA1	1.57	$600 \cdot 10^3$	< 0.2 W/kg (1.5 T-60 Hz)
Metglas 2605CO	1.8	$400 \cdot 10^3$	0.5 W/kg (1.5 T-60 Hz)
Metglas 2605SC	1.61	$300 \cdot 10^3$	0.25 W/kg (1.5 T-60 Hz)
Fe-Ni alloys			
Metglas 2826MB	0.88	$800 \cdot 10^3$	< 120 W/kg (0.7 T-10 kHz)
Co-rich alloys			
Metglas 2714A	0.57	$1000 \cdot 10^3$	< 120 W/kg (0.3 T-100 kHz)
Metglas 2705M	0.77	$600 \cdot 10^3$	< 500 W/kg (0.4 T-100 kHz)

magnetic properties: high permeabilities (up to $600 \cdot 10^3$), high saturation induction (up to 1.8 T) and extremely low specific iron losses (down to 0.2 W/kg at 60 Hz / 1.5 T) [7].

Amorphous materials can be classified in 3 groups [9], characterized by their composition, with different saturation induction levels B_s : (1) Fe-rich alloys with $1.4 \text{ T} < B_s < 1.8 \text{ T}$ for low frequency applications (<1 kHz) (2) Ni-Fe alloys with $0.75 \text{ T} < B_s < 0.85 \text{ T}$ for high frequency applications (up to 100 kHz) and (3) Co-rich alloys with $0.4 \text{ T} < B_s < 1.2 \text{ T}$ mainly used in magnetic sensors and switches (up to 250 kHz). Principal magnetic properties of various Metglas® amorphous alloys from Hitachi Metals are presented in Table I.

Amorphous alloys are made by rapid quenching and produced in ribbons of thickness generally below 40 µm. [9]. Amorphous alloys are among the hardest materials ever made [10]. Metallic glasses are also very brittle especially after thermal treatments (annealing) usually used to improve their magnetic properties. Due to their hardness and brittleness, it is relatively difficult to use conventional cutting or punching manufacturing tools. Laser or chemical cutting methods are more likely to be used.

For these reasons, amorphous materials are commercially available in a limited variety of shapes as toroidally wound or stacked types. Fig 4 shows 2 U-shaped amorphous cores from the Powerlite® products offered by Metglas® [7].

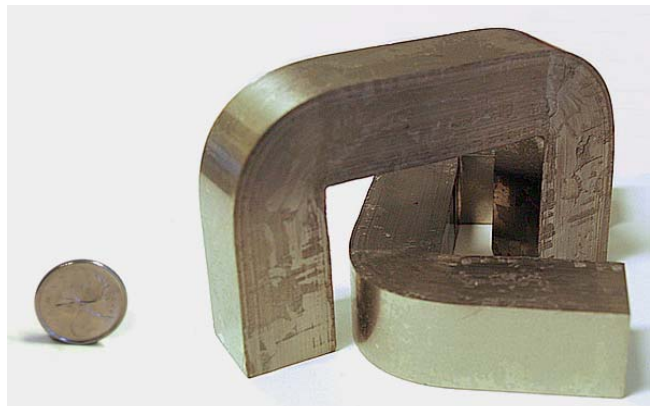


Fig 4: 2 Metglas® Powerlite® amorphous U-shaped cores (AMCC 367S) [7].

One could take profit of the excellent magnetic properties of Fe-rich amorphous alloys for electrical machines. With relatively high saturation inductions, high permeabilities and very low specific iron losses, Fe-rich amorphous alloys can compete with Fe-Si laminations in terms of magnetic properties. Fig 5 compares the AC B-H loops of 2605SA1 Powerlite® Metglas® amorphous cores (Fig 4) to those of M19 0.35 mm-thick lamination stack cores for various frequencies.

Measurements of Fig 5 were made with an AC hysteresigraph using the protocol described in [11], on non-annealed amorphous and lamination stack cores. One can notice the better permeability of the amorphous material over the laminations. As the frequency increases, the amorphous cores exhibit significantly thinner B-H cycles when compared to those of lamination stack cores. This observation let us expect significantly lower eddy current losses occurring in the amorphous cores. Fig 6 compares the iron losses occurring in 2605SA1 Powerlite® Metglas® amorphous cores (depicted in Fig 4) to those occurring in M19 0.35 mm-thick lamination stack cores for 3 different frequencies (60, 400 and 1000 Hz) and at various level of core magnetic flux densities (up to 1.4 T). The measurement protocol is the same as the one described in [11]. Results were obtained with non-annealed cores.

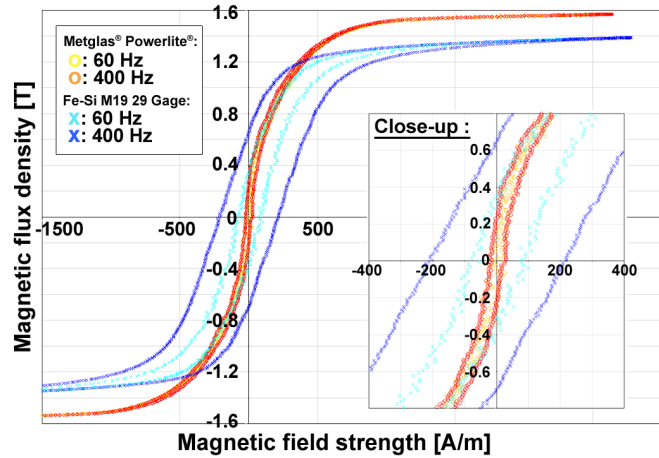


Fig 5: Measured AC B-H loops of 2605SA1 amorphous cores and 0.35 mm - thick (29 Gage) Gage Fe-Si lamination stack cores at various frequencies.

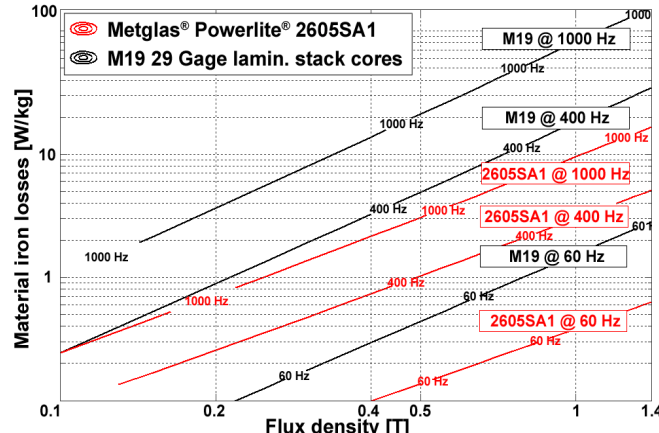


Fig 6: Measured of 2605SA1 amorphous cores (circles) and M19 0.35 mm - thick (29 Gage) Fe-Si lamination stack cores at various frequencies.

Fig 6 shows that the iron losses in the amorphous cores are considerably lower than those occurring in the Fe-Si lamination cores: for example, at 400 Hz and for a core flux density of 1.4 T, 34.5 W/kg are dissipated in the Fe-Si cores whereas the iron losses are around only 5 W/ kg in the amorphous cores, which means near 7 times less.

Industrial applications of soft magnetic amorphous alloys are mainly distribution transformers in low frequencies (below 1 kHz) but also current transformers, sensors and inductors at higher frequencies (up to 250 kHz) [9-11]. Their use in electrical machines is quite seldom. The authors of [9-11] explain this by the high cost of such materials but also because of important manufacturing difficulties: as said before, amorphous metals are thin and brittle and therefore cannot be cut or punch easily to form common motor magnetic circuits.

On the contrary, the CTFM topology with hybrid stator can easily integrate amorphous material with its usual U-core shapes, as a natural replacement to the CTFM laminated C-core. As a consequence, it is possible to take profit of the low-losses properties of amorphous materials by using them in substitution of Fe-Si laminations for the construction of the motor stator C-cores. Amorphous U-shaped cores are commercially available in various sizes, as the Powerlite® cores manufactured by Metglas® [7]. Fig 7 shows one stator pole pair of a CTFM with hybrid stator with an AMCC 367S Metglas® Powerlite® amorphous core (right) instead of the Fe-Si lamination stack core (left) used in [6].

IV. IRON LOSSES IN A CTFM WITH AMORPHOUS CORES

As manufacturing difficulties seems not to be a serious problem in the case of a CTFM with hybrid stator, amorphous stator cores can be favourably used as a substitution of conventional Fe-Si lamination stack cores. The iron loss reduction offered by such materials could improve the motor efficiency and increase its speed range. Experimental measurements and Finite Element Analysis (FEA) were conducted in order to verify these assumptions. The amorphous alloy considered in this study is the 2605SA1 Metglas® alloy.

A. Experimental comparison of iron losses in the stator of a CTFM with amorphous core and with Fe-Si core.

To evaluate the benefits of using amorphous cores in a CTFM with hybrid stator, an experimental setup has been developed. This setup enables evaluating and comparing the iron losses occurring in a CTFM either with amorphous cores

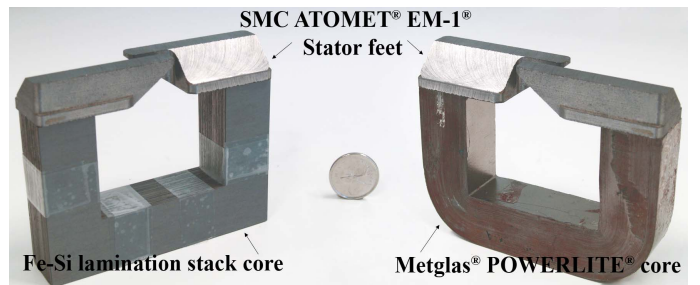


Fig 7: 2 CTFM stator poles with a Fe-Si core (left) and an am. core (right).

or with Fe-Si cores at no-load. Usual methods, such as those based on power loss segregation, are not well suited to our case, being not accurate enough, not adapted to PM motors or giving no information about the iron loss distribution in the motor. The method adopted uses a thermometric approach described in detail in [12]. The principle is as follow:

The iron losses occurring in a machine can be evaluated from the heat they generate. The method used here consists in measuring the initial temperature rise on an insulated stator pole pair. This insulation is a requirement of the developed method, as explained in [12]. A test bench was built to measure the no-load iron losses in the stator (C-core + feet) of a one pole pair CTFM with either a Metglas® Powerlite® (AMCC 367S) amorphous core or an M19 0.35 mm-thick Fe-Si lamination stack core. The latter is shown in Fig 8.

The test rig consists in a 15 pole pairs CTFM rotor mechanically coupled to a DC motor. One pole pair of the CTFM with hybrid stator (C-core + feet), similar as the one depicted in Fig 7, is inserted in the rotor with a thermally insulated fixation unit (Fig 8 bottom-right). The latter is made from PVC and Styrofoam®. As the DC motor rotates, the rotor PM flux flows through the stator pole pair and iron losses are dissipated in the CTFM stator magnetic circuit. Thermocouples are placed on the core and feet in order to measure their temperature rises under PM flux excitation. A coil is used to measure the induction in the core center. Thermocouples are connected to a temperature acquisition unit interfaced to a computer. As explained in [12], the stator iron losses are then calculated from the materials thermal heat capacities and the temperature data.

Losses occurring in the stator C-core (amorphous or Fe-Si) and feet (SMC) were measured for frequencies of the PM flux from 50 Hz to 400 Hz, for a core flux density of 0.4 T and with

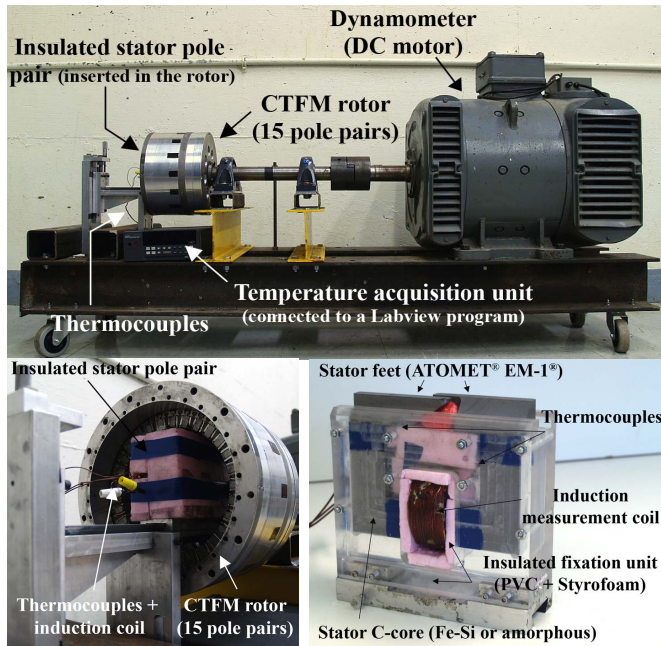


Fig 8: (top): test bench using the insulated thermometric method. (under - left): CTFM close-up. (under - right): Insulated stator pole pair.

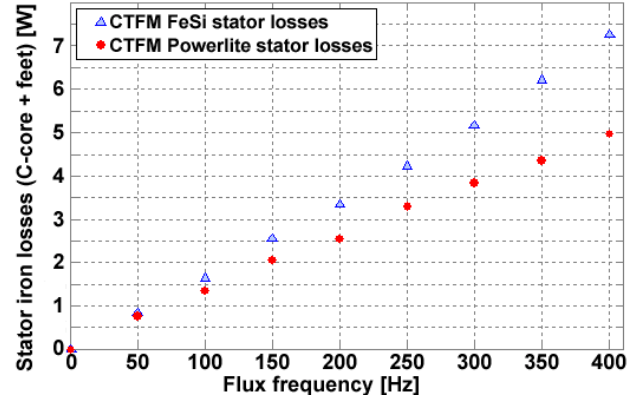


Fig 9: Measurement of total stator iron losses in a one pole-pair CTFM with Fe-Si core (▲) / with a Metglas® Powerlite® amorphous core (●).

no excitation in the stator coil. The iron losses dissipated in the CTFM with the amorphous core are compared to those occurring in the motor with the M19 0.35 mm-thick Fe-Si lamination stack core on Fig 9. The results show a consequent iron loss reduction of up to 30 % of the total stator iron losses in the case of the CTFM with the amorphous core when compared to machine with the Fe-Si core. Measurements for higher core flux densities (> 0.4 T) would certainly have shown greater iron loss reductions. This could have been achieved by reducing the CTFM airgap. Unfortunately, the test rig could not provide airgaps below 2 mm.

From the extremely low-loss performance of amorphous materials presented in the previous section, better iron loss reductions could have been expected. As the machine stator is also made of SMC (feet), it can be supposed that the machine feet exhibit consequent iron losses. In other words, one can expect that the stator iron loss reduction offered by the use of amorphous cores may be limited by an important part of losses occurring in the SMC feet. To verify this assumption, the iron loss distribution between the C-core and feet has to be known.

B. Iron loss distribution in the stator.

The iron loss distribution between the C-core and feet cannot be directly estimated from the developed experimental method. Indeed, the latter enables measuring the total stator losses, without giving information about the contribution of either C-core or feet losses to the total stator losses.

However, the loss distribution can be deduced with the help of analytical formulas. As explained in [6], the flux distribution in the whole C-core is homogeneous. As the C-core section is constant, the core flux density and frequency are measured in the test rig from a coil wound around the core (Fig 8 bottom - right). Flux density and frequency dependent expressions, such as Steinmetz equations, can then be used to estimate the C-core iron losses. The losses dissipated in the amorphous and Fe-Si cores were evaluated with (1) and (2), derived from experimental measurements as detailed in [12]:

$$P_{M19} = m \cdot \left[0.0203 \cdot B_{core}^{1.716} \cdot f + 7.86 \cdot 10^{-5} \cdot B_{core}^2 \cdot f^2 \right] \quad (1)$$

$$P_{Powerlite} = m \cdot \left[0.008 \cdot B_{core}^{1.642} \cdot f + 3.50 \cdot 10^{-6} \cdot B_{core}^2 \cdot f^2 \right] \quad (2)$$

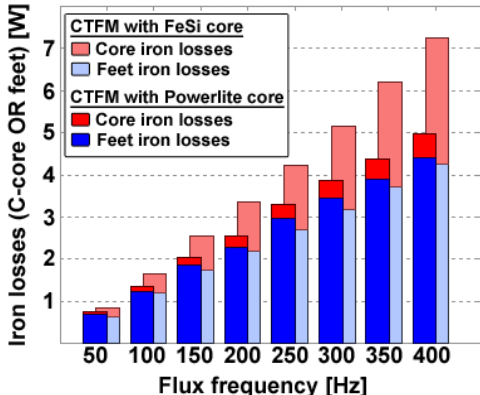


Fig 10: Stator iron losses distribution in the machine core and feet in the one pole-pair CTFM with Fe-Si core (light) / with a Metglas® Powerlite® amorphous core (dark). Bar height is the same in Fig 9.

On the other hand, losses occurring in the feet cannot be calculated in a similar way because the flux distribution in these SMC parts is inhomogeneous. However, the stator feet iron losses can be deduced by subtracting the C-core losses calculated from (1) or (2) to the measured total stator losses (Fig 9). Fig 10 compares the iron losses distribution in the machine core and feet of the CTFM with the amorphous core to the one of the CTFM with the Fe-Si core.

From Fig 10, slight differences can be noticed between the feet losses of the CTFM with the amorphous core and those of the CTFM with the Fe-Si core: although measurements on both cases were made on the same conditions, a maximum difference of 10 % can be observed. This can be explained by the accuracies of the analytical formulas used here. Fig 10 shows above all that the iron losses occurring in the amorphous core represent only a small part (9% to 11%) of the total stator losses. In the case of the CTFM with the Fe-Si core, the proportion of losses in the core is greater and corresponds to 25 % to 41 % of the total stator losses. This observation confirms that the machine feet exhibit important iron losses.

The observations made on experimental results are significant enough to prove the great benefits provided by the use of amorphous cores in a CTFM with hybrid stator. However, it has now been noticed that the major part of the iron losses occurs in the stator feet. Further works should be focused on the iron loss reduction in the CTFM feet.

C. FEA comparison of iron losses in the stator of a CTFM with amorphous core and with Fe-Si core.

FEA simulations were made on a CTFM with amorphous cores and with Fe-Si cores to observe the iron loss reduction in a complete machine. The design used for the simulations is a 10 kW, 3 phases, 15 pole pairs machine similar to the one presented in [6] (30 cm outside diameter, 18 cm airgap diameter, 0.55 mm airgap). Simulations are performed using the 3D FEA package Magnet VI® from Infolytica. Symmetrical boundary conditions are imposed in the calculations, such that only one pole pair of the motor needs to be considered. A sinusoidal magnetomotive force (mmf) of amplitude 3500 A-turns, with a phase shift of 20 degrees with respect to the aligned position, is imposed as done in [6].

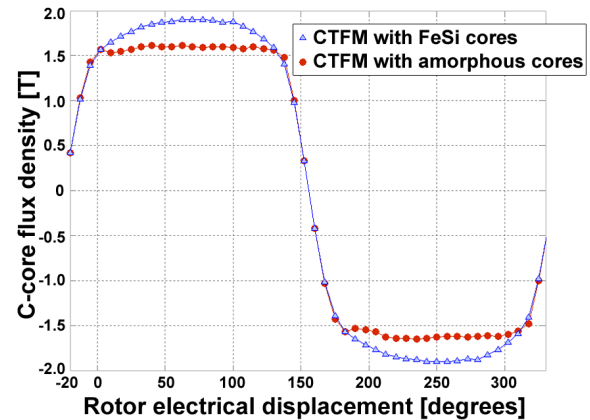


Fig 11: Core flux density waveforms of the CTFM with Fe-Si cores (▲) / with Metglas® Powerlite® amorphous cores (●) computed with FEA.

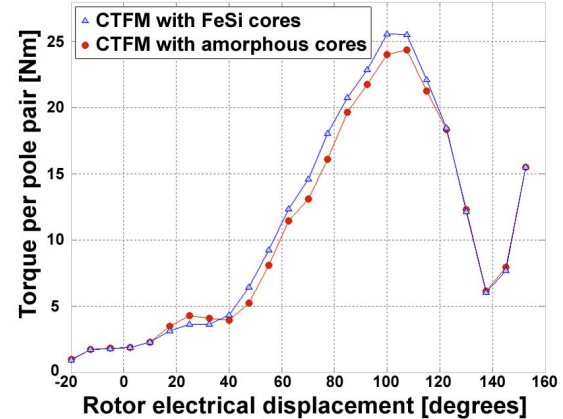


Fig 12: Torque per pole pair waveforms of the CTFM with Fe-Si cores (▲) / with Metglas® Powerlite® amorphous cores (●) computed with FEA.

Flux and torque are computed 24 times in a half cycle of the rotor displacement (every 7.5 electrical degrees). The C-core flux densities for each electrical angle are calculated from the flux data considering a uniform core cross-section. Simulation results for both machines are presented in Fig 11 and Fig 12.

On Fig 11, the shape of the amorphous core flux density waveform indicates that the core saturates at lower flux density: the latter reaches 1.57 T, which corresponds to the saturation induction of the 2605SA1 Metglas® alloy used (Table I). The torque per pole waveforms (Fig 12) are comparable for both machines. Despite the lower saturation induction of the amorphous alloy used, simulation results show that saturation does not greatly affect the machine torque capabilities in this design: a mean torque per pole of 10.4 Nm is achieved by the CTFM with amorphous cores versus 10.9 Nm in the case of the CTFM with Fe-Si cores. Fig 11 and 12 also show that the high permeability of the amorphous alloy does not significantly affect the motor performances.

From the FEA flux density harmonic content, the core iron losses of both machines were evaluated with (3) and (4):

$$P_{FeSi} = m_{core} \cdot \left[0,024 \cdot 1,9^{1.7} \cdot f_i + 6 \cdot 10^{-5} \cdot \left(\sum_{n=1}^{24} B_{ncore}^2 \cdot f_n^2 \right) \right] \quad (3)$$

$$P_{2605SA1} = m_{core} \cdot \left[0,006 \cdot 1,57^{1.465} \cdot f_i + 3,33 \cdot 10^{-6} \cdot \left(\sum_{n=1}^{24} B_{ncore}^2 \cdot f_n^2 \right) \right] \quad (4)$$

Coefficients of (3) and (4) were determined from loss curves obtained from manufacturer data for the M19 0.35 mm-thick Fe-Si laminated steel and from loss measurements for the 2605SA1 Metglas® alloy. These loss curves assume a sinusoidal flux density but Fig 11 clearly shows that the core flux density waveforms are non-sinusoidal. Therefore, the iron loss formulas had to take in account the flux harmonics: in (3) and (4), n is the rank of harmonic considered, m_{core} is the C-core mass, f_n and B_{ncore} are the frequency and amplitude of the flux density for each harmonic contained in the flux waveform. In (3) and (4), hysteresis losses are calculated for the fundamental components only, whereas eddy current losses are associated with the harmonics. The C-core iron losses of both simulated machines are plotted in Fig 13 as a function of motor electrical frequency and speed.

Results of Fig 13 shows that a great iron losses reduction could be achieved in a CTFM by using amorphous cores: a diminution of a factor 7 to 11 of the C-core losses in the case of the CTFM with the amorphous cores when compared to machine with the Fe-Si cores. One can also notice that the loss reduction is greater here than the one observed experimentally (Fig 10), as the core flux density levels are higher.

From these results, the impact of the use of amorphous cores on the CTFM total efficiency has been estimated for various motor electrical frequencies and speeds. Copper losses were estimated to 99 W/ phase [6]. Assumptions were made that the motor mechanical losses vary linearly with the speed. It was also supposed that the iron losses occurring in the SMC parts (stator feet and rotor concentrators) were linearly related to the electrical frequency, as they are mainly hysteresis losses at low frequencies. As the CTFM prototype presented in [6] has the same dimensions and characteristics as the motors simulated here, a linear interpolation from experimental measurements was used to estimate the mechanical and SMC iron losses. The computed efficiencies of both CTFMs are plotted in Fig 14 as a function of the motor frequency and speed.

Fig 14 shows that the CTFM using amorphous cores has a higher efficiency ($> 95.2\% \text{ vs } 92.5\% @ 400 \text{ Hz}$) and is capable of maintaining it over 400 Hz when the other is not. From these results, one can conclude that amorphous cores offer a great loss reduction that could prevent an efficiency

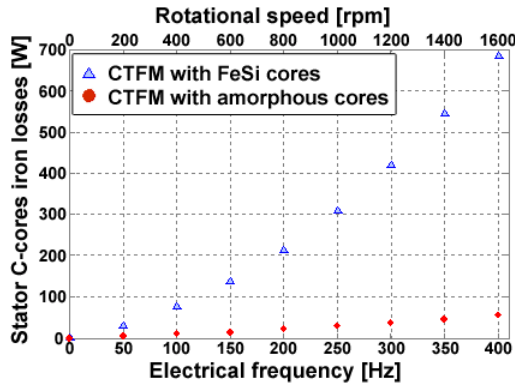


Fig 13: C-core losses prediction computed from FEA results in a 15 pole pairs CTFM with Fe-Si cores (▲) / with Metglas® Powerlite® am. cores (●).

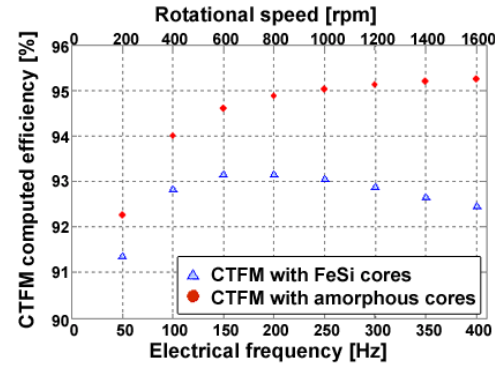


Fig 14: Computed efficiencies of a 15 pole pairs CTFM with Fe-Si cores (▲) / with Metglas® Powerlite® amorphous cores (●).

decrease at higher speeds. By avoiding cooling difficulties, they could also allow using the CTFM at higher frequencies.

V. CONCLUSION

This paper presents a new type of CTFM using a stator built with amorphous cores. The aim of this work was to push further the concept of hybrid stator to reduce the machine iron losses by using a very low-loss magnetic material. It was found that the CTFM topology with hybrid stator can easily integrate amorphous material as a replacement to its laminated C-cores.

The stator iron loss reduction provided by the use of amorphous material has been demonstrated by experimental tests. FEA simulations have also shown a reduction by a factor 7 to 11 of the iron losses occurring in the CTFM C-cores thanks to the use of amorphous cores. It was observed that using amorphous cores in a CTFM could improve the machine efficiency and could allow using this TFM at higher speeds and frequencies. Experimental results finally showed that further works should be focused on reducing the losses in the SMC feet. Full potential of amorphous material will be further exploited and studied soon in a CTFM conception process.

REFERENCES

- [1] Weh H., May H., "Achievable Force Densities for PM Excited Machines in New Configurations", in *Int. Conf. on Elec. Mach. - ICEM*, pp. 1107-1111, Sept. 1986, München, Germany.
- [2] Huang S., Luo J., Lipo T.A., "Analysis and Evaluation of the Transverse Flux Circumferential Current Machine", in *Ind. Appl. Conf. IAS*, Vol. 1, Issue , pp.:378 – 384, 5-9 Oct 1997.
- [3] Viorel I.-A., Henneberger G., Blissenbach R., Löwenstein L., "Transverse Flux Machines. Their Behaviour, Design, Control and Applications", *Mediamira 2003*, Cluj, Romania.
- [4] Maddison C.P., Mecrow B.C. and Jack A.G., "Claw Pole Geometries For High Performance Transverse Flux Machines", *Int. Conf. on Elec. Mach. ICEM*, pp. 340-345, Sept. 98, Vigo, Spain.
- [5] Harris M.R., Pajooman G.H., Abu-Sharkh S.M., "Performance and Design Optimisation of Electric Motors with Heteropolar Surface Magnets and Homopolar Windings", *IEE Proceeding in Elec. Power App.*, vol 143, no. 6, pp 429 – 436, November 1996.
- [6] Dubois M.R., Dehlinger N., Polinder H., Massicotte D., "Clawpole Transverse-Flux Machine with Hybrid Stator", in *Int. Conf. on Elec. Mach. - ICEM*, paper 412, Sept. 2006, Chania, Greece.
- [7] METGLAS, "Powerlite forms, 2605SA1, 2605S3A, 2605CO, 2605SC, 2714A, 2705M, 2826MB", *Technical Bulletins*, www.metglas.com/tech/index.htm [online on June 08].
- [8] Johnson L.A., Cornell E.P., Bailey D.J. and Hegyi S.M., "Applications of low loss amorphous metals in motors and transformers", *IEEE Power Eng. Soc. 1981, Transm. Distr. Conf. Expos.*
- [9] Degauque J., "Matiériaux magnétiques amorphes, micro et nanocrystallins", *Techniques de l'ingénieur, Traité de génie électrique*, 1997, E1170 [In french].
- [10] Ng H. W., Hasegawa R., Lee A. C., Lowdermilk L. A., "Amorphous alloy core distribution transformers", *IEEE Proceeding*, vol. 79, no. 11, November 1991, pp. 1608-1622.
- [11] Cyr C., "Modélisation et caractérisation des matériaux magnétiques composites doux utilisés dans les machines électriques", *PhD Thesis, Université Laval, 2007, Québec Canada* [In french].
- [12] Dehlinger N., Dubois M. R., "A Simple Insulated Thermometric Method for the Experimental Determination of Iron Losses", in *Int. Conf. on Elec. Mach. - ICEM*, Sept. 08, Vilamoura Portugal.